Mechanisms of Vascular Disease:

A Reference Book for Vascular Specialists

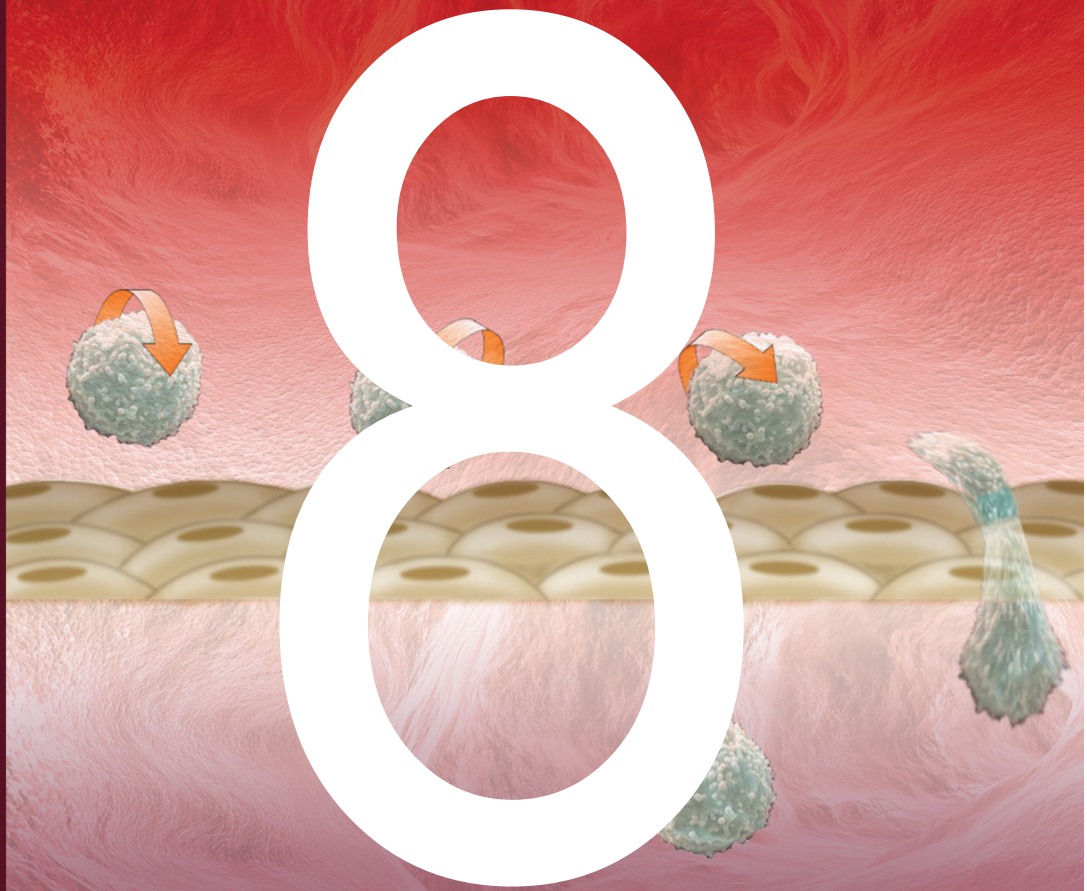

Edited by Robert Fitridge and Matthew Thompson

Completely Updated Edition 2011

Barr Smith Press

Mechanisms of Vascular Disease

Mechanisms of Vascular Disease:
A Reference Book for Vascular Specialists

Robert Fitridge
The University of Adelaide, The Queen Elizabeth Hospital, Woodville, Australia
Matthew Thompson
St George's Hospital Medical School, London, UK

BARR SMITH PRESS
An imprint of
The University of Adelaide Press

Published in Adelaide by

The University of Adelaide, Barr Smith Press
Barr Smith Library
The University of Adelaide
South Australia 5005
press@adelaide.edu.au
www.adelaide.edu.au/press

The University of Adelaide Press publishes peer-reviewed scholarly works by staff via Open Access online editions and print editions.

The Barr Smith Press is an imprint of the University of Adelaide Press, reserved for scholarly works which are not available in Open Access, as well as titles of interest to the University and its associates. The Barr Smith Press logo features a woodcut of the original Barr Smith Library entrance.

This CIP cataloguing for this work is as follows;

Mechanisms of vascular disease : a reference book for vascular surgeons / Robert Fitridge, Matthew Thompson, [editors].

1. Blood vessels, Diseases.
2. Blood vessels, Surgery.

I. Fitridge, Robert
II. Thompson, M. M.

For the full Cataloguing-in-Publication data please contact National Library of Australia:
cip@nla.gov.au

ISBN (paperback) 978-0-9871718-2-5

Book design: Midland Typesetters
Cover design: Emma Spoehr, based on a diagram by Dave Heinrich of the Medical Illustration and Media Unit, Flinders Medical Centre
Paperback edition printed by Griffin Press, South Australia

Table of Contents

List of Contributors

David G Armstrong
The University of Arizona
Southern Arizona Limb Salvage Alliance
Tucson, AZ
USA

Vishwanath Biradar
Intensive Care Unit
The Queen Elizabeth Hospital
Woodville, SA
Australia

Matthew Bown
Department of Vascular Surgery
University of Leicester
Leicester
UK

Andrew W Bradbury
University Department of Vascular Surgery
Birmingham Heartlands Hospital
Birmingham
UK

Edward Choke
Department of Vascular Surgery
University of Leicester
Leicester
UK

Gillian Cockerill
Department of Clinical Sciences
St George's Hospital Medical School
London
UK

Prue Cowled
Department of Surgery
University of Adelaide
The Queen Elizabeth Hospital
Woodville, SA
Australia

Helen Daly
Royal Perth Hospital
Perth, WA
Australia

Mital Desai
University Department of Vascular Surgery
Royal Free Hospital
University College
London
UK

Robert F Diegelmann
Department of Biochemistry
Medical College of Virginia
Richmond, VA
USA

Timothy K Fisher
Rashid Centre for Diabetes and Research
Sheikh Khalifa Hospital
Ajmon
UAE

Robert A Fitridge
Department of Surgery
University of Adelaide
The Queen Elizabeth Hospital
Woodville, SA
Australia

Gail Gillespie
Royal Perth Hospital
Perth, WA
Australia

Jonathan Golledge
Vascular Biology Unit
School of Medicine & Dentistry
James Cook University
Townsville, QLD
Australia

George Hamilton
University Department of Vascular Surgery
Royal Free Hospital
University College
London
UK

Mark Hamilton
Department of Surgery
University of Adelaide
The Queen Elizabeth Hospital
Woodville, SA
Australia

Robert J Hinchliffe
St George's Vascular Institiute
St George's Hospital
London
UK

Richard D Kenagy
Department of Surgery
University of Washington
Seattle, WA
USA

Paul Kerr
Department of Pharmacology
University of Alberta
Alberta
Canada

Michael MD Lawrence-Brown
Curtin Health Innovation Research Institute
Curtin University
Perth, WA
Australia

Brian Lepow
The University of Arizona
Department of Surgery
Southern Arizona Limb Salvage Alliance
Tucson, AZ
USA

Kurt Liffman
CSIRO Material Science & Engineering and School of Mathematical Sciences
Monash University
Melbourne, Vic
Australia

Ian Loftus
Department of Vascular Surgery
St George's Hospital
London
UK

Mark J McCarthy
Department of Surgery and Cardiovascular Sciences
University of Leicester
Leicester
UK

Greg S McMahon
Department of Surgery and Cardiovascular Sciences
University of Leicester
Leicester
UK

Simon McRae
Adult Haemophilia Treatment Centre
SA Pathology
Adelaide, SA
Australia

Joseph L Mills
The University of Arizona
Southern Arizona Limb Salvage Alliance
Tucson, AZ
USA

Lyle Moldawer
Department of Surgery
University of Florida
Gainesville, FL
USA

John L Moran
Faculty of Health Sciences
University of Adelaide
The Queen Elizabeth Hospital
Woodville, SA
Australia

Stephen Nicholls
The Heart and Vascular Institute
Cleveland Clinic
Cleveland, OH
USA

Ian M Nordon
St George's Vascular Institiute
St George's Hospital
London
UK

Paul E Norman
School of Surgery
University of WA
Fremantle, WA
Australia

Karlheinz Peter
Baker IDI Heart & Diabetes Institute
Melbourne, Vic
Australia

Frances Plane
Department of Pharmacology
University of Alberta
Alberta
Canada

Janet T Powell
Imperial College
London
UK

Sandeep Prabhu
Baker IDI Heart & Diabetes Institute
Alfred Hospital
Melbourne, Vic
Australia

Rishi Puri
The Heart and Vascular Institute
Cleveland Clinic
Cleveland, OH
USA

Stephan A Schug
Royal Perth Hospital
Perth, WA
Australia

Gregory S Schultz
Department of Obstetrics and Gynaecology
University of Florida
Gainesville, FL
USA

Rahul Sharma
Baker IDI Heart & Diabetes Institute
Alfred Hospital
Melbourne, Vic
Australia

Guo-Ping Shi
Department of Cardiovascular Medicine
Brigham & Women's Hospital
Harvard Medical School
Boston, MA
USA

Michael Stacey
University Department of Surgery
Fremantle Hospital
Fremantle, WA
Australia

Ilija D Sutalo
CSIRO Material Science & Engineering
and Curtin Health Innovation
Research Instutute
Curtin University
Highett, Vic

Raymond Tam
Department of Pharmacology
University of Alberta
Alberta
Canada

Matthew Thompson
St Georges Hospital Medical School
London
UK

Martin Veller
Department of Surgery
University of Witwatersrand
Johannesburg
South Africa

Mauro Vicaretti
Department of Vascular Surgery
Westmead Hospital
Westmead, NSW
Australia

Matt Waltham
Academic Department of Surgery
St Thomas' Hospital
London
UK

Matthew L White
Vascular and Endovascular Surgery
University of Arizona
Tucson, AZ
USA

David P Wilson
School of Medical Sciences
Discipline of Physiology
University of Adelaide
Adelaide SA
Australia

Qingbo Xu
Department of Cardiology
Kings College
University of London
UK

Detailed Contents

CHAPTER 20 – PATHOPHYSIOLOGY OF PAIN

Stephan Schug, Helen Daly, Kathryn Stannard

CHAPTER 21 – POST-AMPUTATION PAIN

Stephan Schug, Gail Gillespie

CHAPTER 26 – PATHOPHYSIOLOGY AND PRINCIPLES OF MANAGEMENT OF THE DIABETIC FOOT

David Armstrong, Timothy Fisher, Brian Lepow, Matthew White, Joseph Mills

CHAPTER 27 – LYMPHOEDEMA – PRINCIPLES, GENETICS AND PATHOPHYSIOLOGY

Matt Waltham

CHAPTER 28 – GRAFT MATERIALS PAST AND FUTURE

Mital Desai, George Hamilton

Acknowledgements

The Editors gratefully acknowledge the outstanding contributions of each Author involved in this reference book. We would also like to acknowledge the invaluable efforts of Ms Sheona Page who has worked tirelessly on this project. We would also like to thank Prue Cowled PhD and Ms Cayley Wright for their assistance.

Abbreviation List

a1-PI	a1-protease inhibitor
5-HT	5-Hydroxytryptamine/Serotonin
AAA	Abdominal aortic aneurysm
AAS	Acute aortic syndrome
AAV	Adeno-associated viruses
ACE	Angiotensin converting enzyme
ACS	Acute coronary syndrome
ACS	Abdominal compartment syndrome
ACTH	Adrenocorticotropic hormone
ADAMTS	A disintegrin and metalloproteinase with thrombospondin motifs
ADP	Adenosine diphosphate
AIDS	Acquired immune deficiency syndrome
ALI	Acute lung injury
AMP	Adenosine monophosphate
AMPA	α-amino-3 hydroxy-5-methylisoxazole
ANA	Anti-nuclear antibody
ANCA	Anti-neutrophil cytoplasmic antibody
AOD	Aortic occlusive disease
AP1	Activated protein 1
APC	Activated protein C
APC	Antigen presenting cell
APLAS	Antiphospholipid antibody syndrome
ApoAI	Apolipoprotein AI
ApoE	Apolipoprotein E
APS	Antiphospholipid antibody syndrome
APTT	Activated partial thromboplastin time

ARDS	Acute respiratory distress syndrome
AT	Antithrombin
ATP	Adenosine triphosphate
AVP	Ambulatory venous thrombosis
β2-GPI	β2-glycoprotein Ib
bFGF	Basic fibroblast growth factor
BKCa	Large conductance calcium activated potassium channel
BMPs	Bone morphogenetic proteins
BMS	Bare metal stent
CAD	Coronary artery disease
CaM	Calmodulin
CAM	Cell adhesion molecule
cAMP	Cyclic adenosine monophosphate
CCK	Cholecystokinin
cGMP	Cyclic guanine monophosphate
CD	Cluster of differentiation
CD40L	Cluster of differentiation 40 ligand
CEA	Carotid endarterectomy
CETP	Cholesteryl ester transfer protein
CFD	Computational fluid dynamics
CG	Cationized gelatin
CGRP	Calcitonic gene regulated peptide
CHD	Coronary heart disease
CI	Confidence interval
CIMT	Carotid intimal-media thickness
c-JNK	c-Jun N-terminal kinase
CK-MB	Creatinine kinase (Myocardial specific)
CNCP	Chronic noncancer pain
cNOS	Constitutive nitric oxygen synthase enzyme
COX-1	Cyclooxygenase-1
COX-2	Cyclooxygenase-2
CROW	Charcot restraint orthotic walker
CRRT	Continuous renal replacement therapy

CRP	C-reactive protein
CRPS	Complex regional pain syndromes
CT	Computational tomography
CTA	Computed tomographic angiography
CTD	Connective tissue disorders
CTGF	Connective tissue growth factor
CYP	Cytochrome P450
CVD	Cardiovascular disease
CVI	Chronic venous insufficiency
DAG	Diacylglycerol
DES	Drug-eluting stent
DRG	Dorsal root ganglion
DNA	Deoxyribonucleic acid
DSA	Digital subtraction arteriography
DTS	Dense tubular system
DVT	Deep vein thrombosis
EC	Endothelial cell
ECM	Extracellular matrix
EDCF	Endothelium-derived contracting factor
EDH	Endothelium-dependent hyperpolarisation
EDS	Ehlers-Danlos syndrome
EET	Epoxyeicosatrienoic acids
ELAM-1	Endothelial-leukocyte adhesion molecule-1
ELG	Endoluminal grafts
ELISA	Enzyme linked immunosorbent assay
E_K	Equilibrium potential
E_M	Membrane potential
eNOS	Endothelial nitric oxide synthase enzyme
EPC	Endothelial progenitor cells
EPCR	Endothelial protein C receptor
ePTFE	Expanded polytetrafluoroethylene
ERK	Extracellular signal-regulated kinase
ESR	Erythrocyte sedimentation rate

ET	Essential thrombocytosis
ET-1	Endothelin 1
EVAR	Endovascular aortic aneurysm repair
EVLA	Endovenous LASER ablation
FDA	Food and drug administration
FDPs	Fibrin degradation products (soluble)
FGF	Fibroblast growth factor
FGF-2	Fibroblast growth factor 2
FMN	Flavin mononucleotide
FVL	Factor V Leiden
GABA	Gamma-aminobutyric acid
GABA B	Gamma-aminobutyric acid subtype B
G-CSF	Granulocyte colony stimulating factor
GMCSF	Granulocyte-macrophage colony stimulating factor
GP	Glycoprotein
GPCR	G-protein coupled receptor
GSV	Great saphenous vein
HDL	High density lipoprotein
HDL-C	High density lipoprotein cholesterol
HIF	Hypoxia inducible factor
HIT	Heparin induced thrombocytopenia
HIV	Human immunodeficiency virus
HLA	Human leukocyte antigen
HMG Co-A	Hydroxymethylglutaryl coenzyme-A
HMW	High molecular weight
HPETE	Hydroperoxyeicosatetraenoic acid
HETE	Hydroxyeicosatetraenoic acids
HR	Hazard ratio
hsCRP	High-sensitive C-reactive protein
HSP	Heat shock protein
HUV	Human umbilical vein
IAH	Intra-abdominal hypertension

IAP	Intra-abdominal pressure
IAPP	Intra-abdominal perfusion pressure
ICAM-1	Inter-cellular adhesion molecule-1
ICAM-2	Inter-cellular adhesion molecule-2
ICP	Intra-compartmental pressure
ICU	Intensive care unit
IFN	Interferon
IGF-1	Insulin-like growth factor-1
IHD	Ischemic heart disease
IL	Interleukin
IL-1	Interleukin-1
IL-1α	Interleukin-1 alpha
IL1-β	Interleukin-1 beta
IL-6	Interleukin-6
IL-8	Interleukin-8
ILT	Intraluminal thrombus
IKCa	Intermediate conductance calcium-activated potassium channels
IMH	Intramural haematoma
IMP	Inosine monophosphate
iNOS	Inducible nitric oxide synthase enzyme
IP(3)	1,4,5-inositol triphosphate
IRI	Ischemia reperfusion injury
IVIG	Intravenous pooled immunoglobulin
IVUS	Intravascular ultrasound
KGF	Keratinocyte growth factor
KGF-2	Keratinocyte growth factor-2
LAP	Latency associated peptide
LCS	Limb compartment syndrome
LDL	Low density lipoprotein
LDS	Loeys-Dietz syndrome
LLC	Large latent complex
LEC	Lymphatic endothelial cells

LFA-1	Lymphocyte function-associated antigen-1
LO	Lipoxygenase
LOX	Lysyl oxidase
LOPS	Loss of protective sensation
LPA	Lysophosphatidic acid
LPS	Lipopolysaccharide
LTA	Lipoteichoic acid
LTGFBP	Latent TGF binding protein
MAC-1	Macrophage-1 antigen
MAPK	Mitogen activated protein kinase
MCP-1	Monocyte chemoattractant protein-1
M-CSF	Macrophage-colony stimulating factor
MFS	Marfan syndrome
MHC	Major histocompatibility
MI	Myocardial infarction
MIP-1	Macrophage inflammatory protein-1
MLC_{20}	Myosin light $chain_{20}$
MLCK	Myosin light chain kinase
MLCP	Myosin light chain phosphatase
MMP	Matrix metalloproteinase
MODS	Multiple organ dysfunction syndrome
MRA	Magnetic resonance angiography
MRI	Magnetic resonance imaging
mRNA	Messenger RNA
MRSA	Methicillin resistant *Staphylococcus aureus*
MRSE	Methicillin resistant *Staphylococcus epidermidis*
MRTA	Magnetic resonance tomographic angiography
MTHFR	Methylenetetrahydrofolate reductase
MT-MMP	Membrane-type MMP
MVPS	Mitral valve prolapse syndrome
NADPH	Nicotinamide adenine dinucleotide phosphate
NGF	Nerve growth factor

NFκB	Nuclear factor kappa B
NiTi	Nitinol
NJP	Non-junctional perforators
NMDA	N-methyl-D-aspartate
NNH	Number needed to harm
NNT	Number needed to treat
NO	Nitric oxide
NOS	Nitric oxide synthase enzyme
NSAID	Non-steroidal anti-inflammatory drug
NV	Neovascularisation
OCP	Oestrogen/progesterone contraceptive pill
OPN	Osteopontin
OPG	Osteoprotegerin
OR	Odds ratio
OxLDL	Oxidised low density lipoprotein
PAD	Peripheral arterial disease
PAF	Platelet activating factor
PAI	Plasminogen activator inhibitor
PAI-1	Plasminogen activator inhibitor-1
PAR	Protease activated receptor
PAR-1	Protease activated receptor-1
PAR-4	Protease activated receptor-4
PAU	Penetrating aortic ulcer
PC	Protein C
PCA	Poly (carbonate-urea) urethane
PCI	Percutaneous coronary intervention (angioplasty)
PCWP	Pulmonary capillary wedge pressure
PDGF	Platelet-derived growth factor
PDGFβ	Platelet-derived growth factor-β
PDS	Polydioxanone
PECAM-1	Platelet-endothelial cell adhesion molecule-1
PEDF	Pigment epithelium-derived factor
PES	Paclitaxel-eluting stent

PET	Positron emission tomography
PF4	Platelet factor 4
PGI_2	Prostacyclin
PGG_2	Prostaglandin G_2
PGH_2	Prostaglandin H_2
$PGEI_2/PGI_2$	Prostaglandin I_2
PGN	Peptidoglycan
PHN	Postherpetic neuropathy
PHZ	Para-anastomotic hyper-compliant zone
PI3K	Phosphatidylinositol 3-kinase
PIP2	Phosphatidylinositol 4,5-bisphosphate
PLC	Phospholipase C
PLOD	Procollagen lysyl hydroxylase
PMCA	Plasma membrane Ca^{2+} APTases
PMN	Polymorphonuclear leukocyte
POSS	Polyhedral oligomeric silsesquioxanes
PPAR	Peroxisomal proliferation activating receptor
PPI	Proton pump inhibitor
PRV	Polycythaemia rubra vera
PS	Protein S
PSGL-1	P-selectin glycoprotein ligand-1
PT	Prothombin time
PTCA	Percutaneous coronary angioplasty
PTFE	Polytetrafluoroethylene
PTS	Post-thrombotic syndrome
PUFA	Polyunsaturated fatty acid
PVI	Primary valvular incompetence
rAAA	Ruptured AAA
Rac	Ras activated cell adhesion molecule
RANTES	Regulated upon activation, normal T cell expressed and secreted
RAS	Renin angiotensin system
RCT	Randomised controlled trial

RF	Rheumatoid factor
RFA	Radiofrequency ablation
rhAPC	Recombinant human activated protein C
RNA	Ribonucleic acid
ROS	Reactive oxygen species
RR	Relative risk
RSD	Reflex sympathetic dystrophy
S1P	Sphingosine-1-phosphate
SAPK	Stress-activated protein kinase
SCF	Stem cell factor
SCS	Spinal cord stimulation
ScvO2	Superior vena cava venous oxygen saturation
SDF-1	Stromal-cell-derived factor-1
SERCA	Sarco/endoplasmic reticulum CaATPases
SEP	Serum elastin peptides
SES	Sirolimus-eluting stent
SEPS	Subfascial endoscopic perforator surgery
SFA	Superficial femoral artery
SFJ	Sapheno-femoral junction
SIRS	Systemic inflammatory response syndrome
SKCa	Small conductance calcium-activated potassium channels
SLE	Systemic lupus erythematosus
SMA	Smooth muscle alpha actin
SMC	Smooth muscle cell
SMP	Sympathetically maintained pain
SNARE	Soluble N-ethylmaleimide-sensitive factor activating protein receptors
SNP	Single nucleotide polymorphisms
SNRI	Serotonin/Noradrenaline reuptake inhibitors
SPJ	Sapheno-popliteal junction
SPP	Skin perfusion pressure
SR	Sarcoplasmic reticulum
SSRIs	Selective serotonin re-uptake inhibitors
SSV	Small saphenous vein

SVT	Superficial thrombophlebitis
STIM1	Stromal interacting molecule 1
TαCE	TNFα converting enzyme
TAAD	Thoracic aortic aneurysm disease
TAD	Thoracic aortic dissection
TAFI	Thrombin-activatable fibrinolysis inhibitor
Tc-99 MDP	Technetium-99 methylene diphosphonate
TCA	Tricyclic antidepressant
TCC	Total contact cast
TCR	T-cell receptor
TENS	Transcutaneous electrical nerve stimulation
TF	Tissue factor
TFPI	Tissue factor pathway inhibitor
TGF	Transforming growth factor
TGF-α	Transforming growth factor-alpha
TGF-β	Transforming growth factor-beta
TGL	Triglycerides
Th	T helper
TIA	Transient ischemic attack
TIMP	Tissue inhibitors of metalloproteinase
TLR	Toll-like receptors
TNF	Tumour necrosis factor
TNF-α	Tumour necrosis factor-alpha
tPA	Tissue-type plasminogen activator
TRP	Transient receptor potential
TRPC	Transmembrane receptor potential canonical
TRPV1	Transmembrane receptor potential Vanilloid-type
TXA2	Thromboxane A2
uPA	Urokinase
UT	University of Texas
VCAM	Vascular cell adhesion molecule
VCAM-1	Vascular cell adhesion molecule-1
VEGF	Vascular endothelial growth factor

VEGF-R	Vascular endothelial growth factor receptor
VIP	Vasoactive intestinal peptide
VLA-1	Very late activating antigen-1
VOCC	Voltage operated calcium channels
VPT	Vibratory perception threshold
VSMC	Vascular smooth muscle cells
VTE	Venous thromboembolism
VV	Varicose veins
vWF	von Willebrand factor
XO	Xanthine oxidase

8 • Vascular Arterial Haemodynamics

MICHAEL MD LAWRENCE-BROWN[1], KURT LIFFMAN[1,2,3]
JAMES B SEMMENS[1], ILIJA D SUTALO[1,2]

[1]Curtin Health Innovation Research Institute, Curtin University, Perth, Western Australia, Australia

[2] Materials Science and Engineering, Commonwealth Scientific and Industrial Research Organisation (CSIRO), Highett, Victoria, Australia

[3] School of Mathematical Sciences, Monash University, Victoria, Australia

INTRODUCTION

Vascular interventions have developed rapidly since the first aortic replacement with Dacron by Dubois in 1952. Understanding vascular haemodynamics and the biological response to implanted materials is essential for vascular surgeons and scientists developing new interventional technologies.[1,2]

This chapter will summarise and discuss the following laws, equations and phenomena to give a basic understanding of the haemodynamic principles of the conduits and fluids with which we work:

- Laplace's law of wall tension
- Newtonian Fluid
- Non-Newtonian fluid
- Poiseuille Flow
- Bernoulli's equation
- Young's modulus and pulsatile flow
- Mass conversation
- Reynolds' number: laminar and turbulent flow
- Shear stress and pressure
- Forces on graft systems
- Computational modelling

For those who understand electrical circuit theory, there is much similarity with haemodynamics. Understanding the physiology and physics of blood flow is aided by the use of that recognition. When considering fluid dynamics instead of:

$$V = IR, \tag{1}$$

where V is the voltage, I is the current and R is the electrical resistance. This formula maybe substituted by:

$$P = QR, \tag{2}$$

with P the pressure, Q the volume flow rate and R the flow resistance.

Resistors in series and parallel govern degrees of ischaemia and the behaviour of blood flow and contribution of collaterals, and hence degree of ischaemia of limbs and organs.

The great vessels, like the aorta, are without muscle and their walls are composed of collagen and elastin fibres. This allows them

to behave as capacitors and store some of the energy in systole to be released to power flow in diastole, that is so important *into* vessels such as the coronary artery. The elastic arteries stiffen with age and explain the flow changes that occur with ageing and for progressive arterial disease due to this most important of all the risk factors.

LAPLACE'S LAW OF WALL TENSION

Laplace's law relates the tension in an arterial or venous wall with the pressure that the elastic tube can apply to material inside the tube. To assist in understanding this law we consider Figure 8.1. In this figure, w, represents the thickness of the arterial wall, r is the inner radius of the artery, P the inward pressure force due to the elastic nature of the artery and T is tensional stress within the wall of the vessel, where the tensional stress points in a direction that is tangential to the vessel wall. Due to mass conservation the wall thins as the vessel expands.

The formula for Laplace's law is given by the Eq.:

$$P = \frac{w}{r} T, \tag{3}$$

where it is usually assumed that the wall thickness, w is small relative to r. This law tells us that the inward pressure that is exerted by the vessel wall on the blood is directly proportional to the tensional stress in the wall and inversely proportional to the radius of the wall. Thus the smaller the vessel the larger the pressure it can apply on the blood.

Large thin-walled vessels are low pressure vessels. Increasing the pressure distends the vessel and increases the vessel volume which is a characteristic property of veins. For arteries to maintain pressure, the width of the wall must obviously be greater, so large veins are thin-walled and arteries are thick-walled.

One consequence of this behaviour is that, to a certain extent, an artery acts like a long cylindrical party balloon. When one attempts to blow up such a balloon, it is quite difficult to do at the first blow, however once the balloon reaches a particular radius, it usually becomes much easier to expand the balloon. That is you require less pressure to increase the size of the balloon. This phenomenon is known as instability. If this happens to an artery, then we are dealing with an aneurysm and the relatively constant blood pressure will keep on increasing the size of the aneurysm.

The radius of the artery at which this instability occurs is difficult to compute accurately, but some fairly general arguments suggest that the following formula is a good guide: where r_c is the critical radius for the onset

$$r_c \sim 2r_0, \tag{4}$$

of the instability and r_0 is the initial radius of the artery. The median diameter of the aorta is 23 mm and the thus aortic rupture is very rare when less than 50 mm in diameter, which is consistent with recent clinical

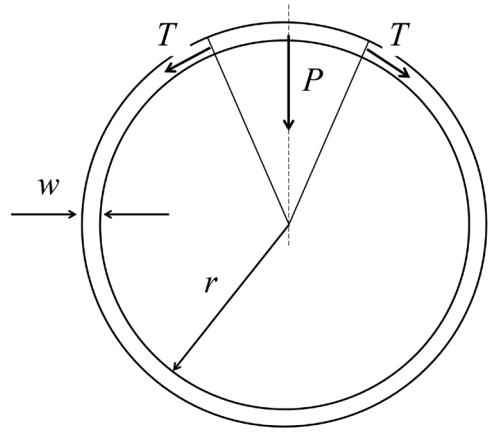

FIGURE 8.1: Cross section of an artery showing the various physical components that make up Laplace's law.

data.[3,4] This guide also directs us to consider that the ratio of the diameters is probably more important than the absolute diameter and this should be taken into account when assessing aneurysms in the smaller diameter vessels of women. How arterial wall instability arises is illustrated in Figure 8.2, where in Figure 8.2(a) we show the stress structure within a small artery. Here the tensile stresses have a component in the radial direction, where the letter T labels this component. In Figure 8.2(b) the aneurysm/balloon has become very large, such that over a small segment of the wall the artery has hardly any curvature. This is an extreme case, but it does show that there is now no radial component to the tensile stresses. In such a case, the aneurysm can expand freely for just about any internal arterial pressure.

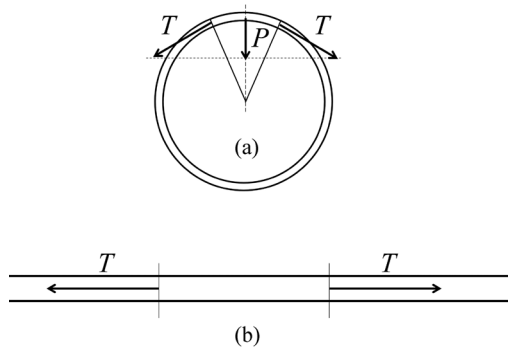

FIGURE 8.2: Cross sections of a small artery (a) and a very large artery (b) showing the stress distribution within the artery.

NEWTONIAN FLUID

When we wish to describe the behaviour of a fluid it is necessary to know something about the frictional properties of the fluid. Consider the schematic depiction of a fluid shown in Figure 8.3. In this figure, fluid is flowing from left to right along the x direction. For purposes of illustration, we assume that the speed of the fluid, u, is increasing with increasing height (*i.e.*, increasing y). This means that elements of fluid are sliding past each other and so generate some frictional stress τ. In a Newtonian fluid, the frictional stress is proportional to the rate at which the speed changes as a function of distance, where μ is the viscosity (Eq (5)). The du/dy in equation (5) corresponds to the shear rate. To a reasonable approximation, one can assume that blood is a Newtonian fluid, at least for flow along the major arteries.

$$\tau = \mu \frac{du}{dy}, \tag{5}$$

NON-NEWTONIAN FLUID

Non-Newtonian fluids have a viscosity that depends on the strain rate. A shear thinning fluid is a fluid that changes from "thick" to "thin" when force is applied to the fluid. Examples of such fluids are shampoos and paints. This behaviour usually occurs, because, at rest, a shear thinning fluid typically has a tangled molecular structure, which makes the fluid relatively viscous. When force is applied, the molecules become ordered, the fluid viscosity decreases and the fluid begins to flow more easily. In Figure 8.4 we show the experimentally determined shear thinning behaviour of blood, where the hematocrit value for the blood is 45%. These data show that for high shear rates, which may occur in the large arteries of the body, the viscosity of blood is about four times that of water (where the viscosity of water is approximately one centipoise (cP)). However for lower shear rates, the viscosity of blood can be over one hundred times that of water.

This change in viscosity is mostly due to the collective behaviour of red blood cells. At low shear rates, red blood cells form aggregates where they stack one upon another, somewhat like a cylindrical pile of coins. These "stacks" of red blood cells are known

as "rouleaux" (Figure 8.5). When the shear rate increases, these aggregates of blood cells are broken down and the blood viscosity decreases. For high shear rates, the blood cells tend to become elongated and line up with the flow of the liquid. This also tends to decrease the viscosity of the blood.

Given that the viscosity of blood increases with decreasing shear, one would think that the viscosity of blood within the body should increase as blood travels from the arteries through the arterioles and into the capillaries. This is because the shear rate and velocity of the blood decreases as the blood travels from the arteries through to the capillaries. The viscosity of blood, however, may be approximately constant throughout much of the body. This

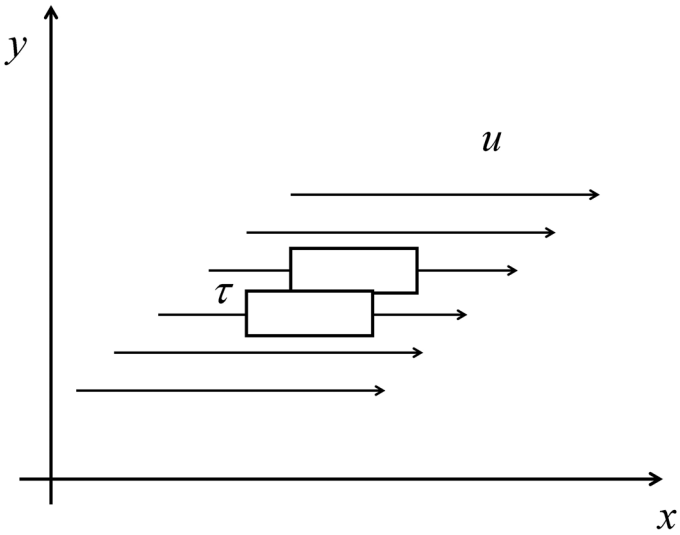

FIGURE 8.3: Elements of fluid slide past each other and generate a frictional shear stress.

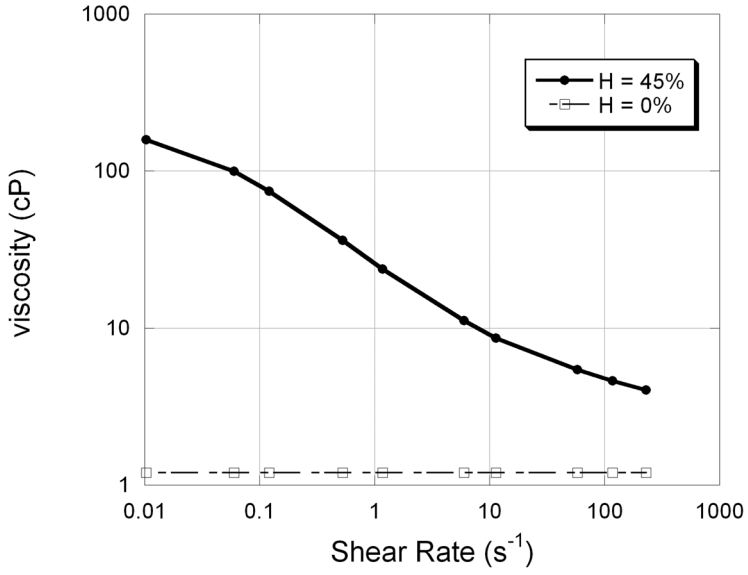

FIGURE 8.4: Blood viscosity as a function of shear rate for 0% and 45% hematocrit.[5]

effect arises due to separate physical flow phenomena:

First, the viscosity of blood is dependent on the hematocrit. If the hematocrit decreases then the blood viscosity decreases. For example in Figure 8.4 we show the viscosity of blood as a function of shear rate for 45% and 0% hematocrit. For 0% hematocrit line the viscosity of the blood is constant and has a value of approximately 1.6 cP.

Second, the hematocrit level is dependent on the diameter of the blood vessel. As the blood vessel decreases in diameter, the hematocrit level also decreases (Figure 8.6). This effect occurs because the blood cells tend to move away from the vessel walls and travel where the flow velocity is a maximum. This behaviour is known as the Fahraeus Effect and it has been shown to occur in tubes with a diameter as small as 29 μm.[6,7] Given that a blood cell has a diameter of around 8 μm it is possible that the Fahraeus Effect may occur in tubes with diameters less than 29 μm.

The combination of these two effects implies that the viscosity of blood is approximately constant throughout the body. Understanding these properties affects the thinking of shear stress between blood and

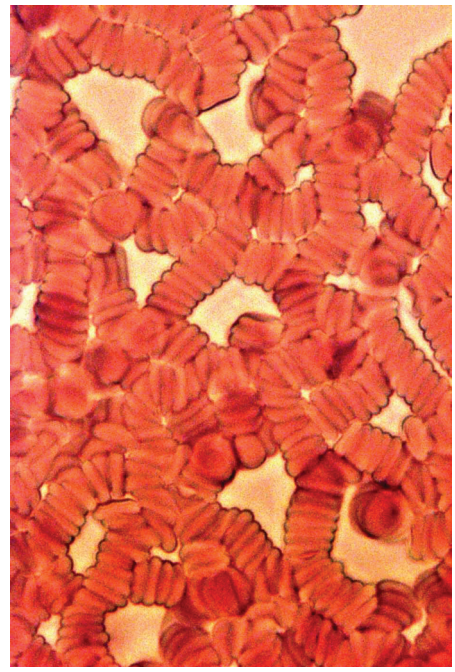

FIGURE 8.5: Rouleaux blood cell network.

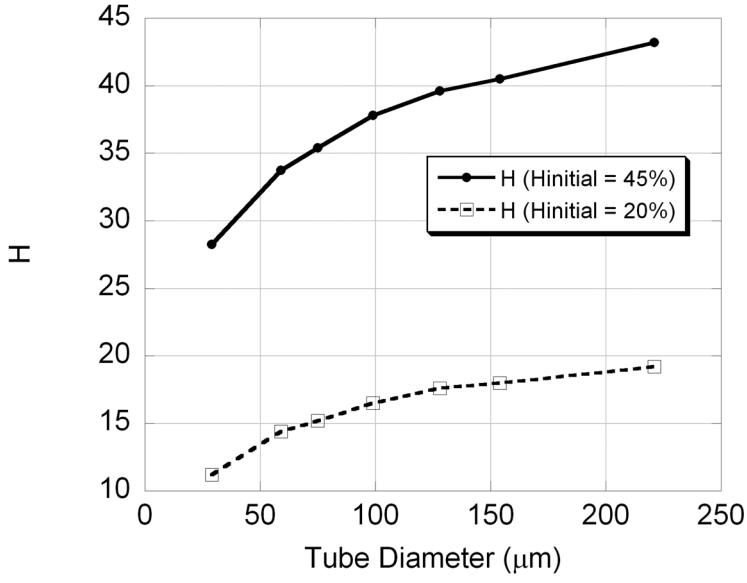

FIGURE 8.6: Hematocrit as a function of tube diameter. The initial hematocrit value for each line is shown in the inset box[8].

vessel walls – or more relevantly between blood and atheroma.

POISEUILLE FLOW

Suppose that you have a Newtonian fluid flowing, in a steady, non-pulsatile manner, down a cylindrical, non-elastic pipe of length L and radius a. If the pipe is long enough, the flow will develop a parabolic velocity profile, which is generally called a Poiseuille flow profile (Figure 8.7). The flow takes its name from Jean Louis Poiseuille, a physician with training in physics and mathematics, who first described the flow structure in 1846.

The volumetric flow rate (q) for Poiseuille flow, *i.e.*, the volume of fluid flowing along the tube per unit time is given by the formula

$$q = \frac{(p_1 - p_2)\pi a^4}{8\mu L}, \qquad (6)$$

where $p_1 - p_2$ is the pressure difference between the two ends of the tube and μ is the viscosity of the fluid.

The physics of the flow is nicely described by this equation. That is, flow is driven by the pressure gradient in the tube or conversely, when there is flow in a tube then you must have a pressure gradient to drive the flow.

Prostheses are subject to the intermittent forces of pulsation and flow. The large elastic vessels are capacitors and provide onflow in diastole and the muscular peripheral vessels maintain pressure by altering resistance mediated via physiological feedback. Current prostheses are not able to do this and have to withstand the forces.

Note also the parameter of length. Flow is therefore also related to length. Patency, such as in femoro-popliteal synthetic conduits, maybe as much, if not more, related to length of conduit as it is to angulation across bend points depending on the haematological factors depositing thrombus. This may also partly explain better patency in shorter bypass grafts.

BERNOULLI'S EQUATION

Johann Bernoulli (1667–1748) was a professor in Basel and taught physics, anatomy and physiology and his understanding lies at the heart of vascular physics and relates pressure to motion and energy. For a fluid that has no viscosity, one can write

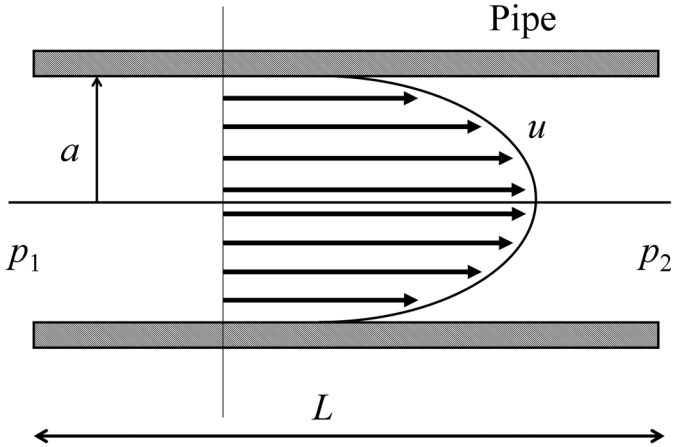

FIGURE 8.7: Parabolic velocity profile for fully developed Poiseuille flow.

$$p + \rho\frac{u^2}{2} + \rho gy = \text{constant of the flow,} \qquad (7)$$

where p is the pressure, ρ the mass density of the liquid, u the speed of the fluid, g the gravitational acceleration, and y the height. In other words, the Bernoulli equation states that the pressure plus the kinetic energy per unit volume, $\rho\frac{u^2}{2}$, plus the potential energy per unit volume, ρgy, is a constant at any point along the blood vessel. So for a constant height, an increase in flow speed implies a decrease in pressure, while for constant flow speed, an increase in height implies a decrease in pressure.

It should be understood that Eq. (7) is an approximation, as it ignores the loss of energy due to shearing friction between the flowing blood and the walls of the artery. Even so, it does provide us with an intuitive understanding of the physics of the arterial/venous system. For example, suppose we wish to measure the blood pressure of a person. Typically one places a sleeve or an external cuff around the upper arm. The upper arm is chosen because it is at approximately the same level of the heart and so the pressure will not be affected by any difference in height. To measure the systolic pressure, the cuff pressure is increased until all blood flow ceases from Eq. (7) we know that this "cut-off" pressure is the maximum pressure in the artery. The pressure in the external cuff is then decreased until the flow is a maximum. We then know that the pressure will be a minimum and this is the diastolic pressure in the artery.

In practice, the arterial system has two sources of potential energy to drive the blood forward. The first is blood pressure and this is transformed into kinetic energy of flow during the period between systole and diastole, and the second is stored energy in the wall of the artery – its capacitance. Consider what might happen when the kinetic energy meets a resistive obstacle – some energy is dissipated as heat as with circuit theory and some is stored for use in diastole for onward flow in the period of heart filling by the elasticity of the great vessels acting as a capacitor. However, some energy is used up as a water hammer. The repetitive alterations in forward pressure and resistive back-pressure with pulsatile flow in a physiologically responding, pressurized system sets up the potential for the water hammer. The injury and healing cycle effect of these water hammers on atherogenesis and aneurysm behaviour at stress points has yet to be fully determined.

YOUNG'S MODULUS AND PULSATILE FLOW

Blood flows through the arteries in a pulsatile fashion. Arteries are semi-elastic tubes and the arteries expand and contract as the pulse of blood flows along the artery. The speed, c, at which blood flows along an artery is determined by the speed that a pulse of fluid can travel along an elastic tube. This speed is given, approximately, by the Moen-Korteweg formula:

$$c \approx \sqrt{\frac{Eh}{\rho d}}, \qquad (8)$$

where E is Young's modulus for the wall of the artery, h is the thickness of the artery, d is the inner diameter of the artery and ρ is the density of blood. A schematic depiction of how a pulsatile wave propagates along an artery is given in Figure 8.8.

As can be seen from Eq. (8), the speed at which blood travels along an artery is partially dependent on the Young's Modulus of the arterial wall. To illustrate the definition of Young's Modulus it is useful to consider Figure 8.9, where a block of material is being stretched due to an applied force on one end of the block.

The block has a natural length denoted by L, when a force F is applied to one side of the block then the length of the block increases by ΔL. This change in length is known as a *strain*, ε, and it is defined by the equation

$$\varepsilon = \frac{\Delta L}{L}. \tag{9}$$

The *stress* that the force applies to the block of material has the definition

$$\sigma = \frac{F}{A}. \tag{10}$$

Young's Modulus is defined as the stress over the strain, *i.e.*,

$$E = \frac{\sigma}{\varepsilon}. \tag{11}$$

Young's modulus is a measure of how easy it is to stretch and compress a material. Thomas Young (1773 – 1829) was a medical physician who made significant contributions to fields of Physics (through his experiments which demonstrated the wave-like nature of light), linguistics (via his identification of the Rosetta Stone), medicine (with his studies of blood flow), and structural mechanics (*e.g.*, Young's Modulus). He was well aware of

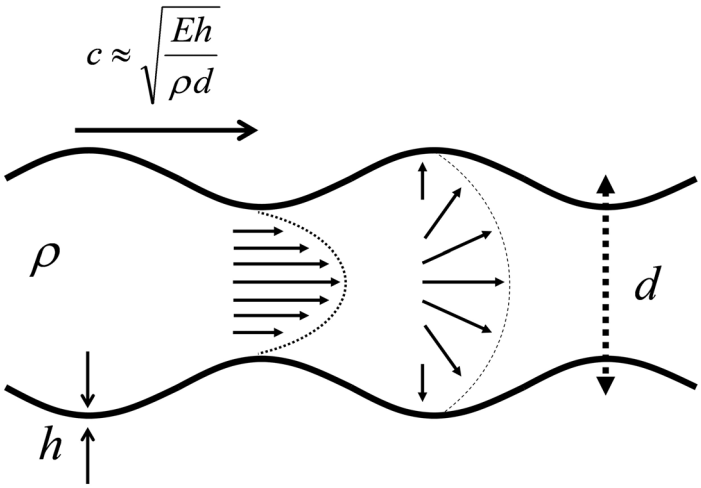

FIGURE 8.8: An exaggerated, schematic view of blood flow in an artery.

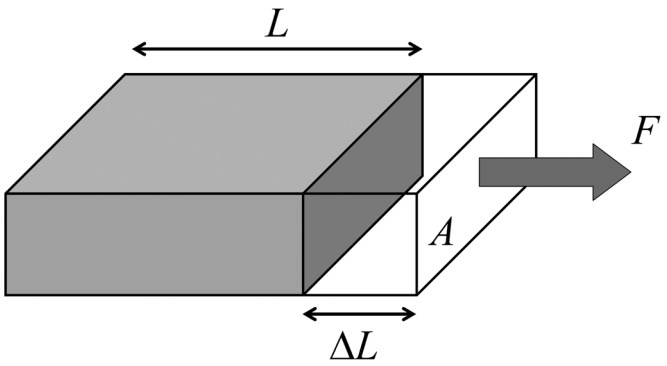

FIGURE 8.9: A block of material with a length, L, and side area A is subject to a force F. The applied force stretches the block a distance ΔL.

the elastic nature of arteries, but, somewhat ironically, does not appear to have used Young's Modulus to describe their properties.

One consequence of aging is increasing stiffness in the arteries. This means that the Young's modulus increases and this, as a consequence of Eq. (8), increases the speed of pulsatile flow within the arterial system.

MASS CONVERSION

In Figure 8.10 we view a schematic depiction of an artery that is changing in shape as one travels along the artery. The blood flows in at one end with a speed u_1. The area at the inlet of the artery is given by A_1. In its simplest form, the mass conservation equation provides us with the relationship between the quantities at the proximal and distal ends of the artery:

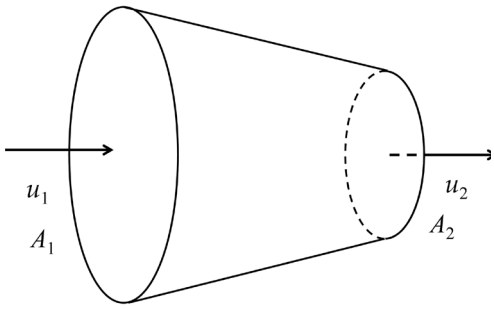

FIGURE 8.10: A change in the diameter of an artery leads to a change in the blood flow speed.

$$u_1 A_1 = u_2 A_2, \tag{12}$$

here u_2 and A_2 are the outlet flow speed and area, respectively. In plain English, Eq. (12) is another way of saying "what goes in must come out".

We can see from Eq. (12) that if an artery becomes narrower, i.e., A_2 becomes smaller, then the flow speed, u_2, increases. This occurs because the mass flow is conserved and so if the tube becomes narrower then the flow rate has to increase.

Some diseased blood vessels develop a constriction or stenosis (Figure 8.11). This narrowing of the blood vessel wall may be caused by atherosclerosis or neo-intimal hyperplasia after an intervention. If we assume steady-state, Newtonian blood flow and ignore gravity then the pressure in a compromised blood vessel with a stenosis can be calculated by combining Bernoulli's equation (equation 7) and the mass conservation (equation 12) to obtain

$$p_1 + \frac{\rho v_1^2}{2} = p_2 + \frac{\rho}{2}\left(\frac{v_1 A_1}{A_2}\right)^2, \tag{13}$$

$$p_2 = p_1 + \frac{\rho v_1^2}{2}\left(1 - \left(\frac{A_1}{A_2}\right)^2\right). \tag{14}$$

Since $A_2 < A_1$ the energy last term of equation 14 becomes negative so then the blood

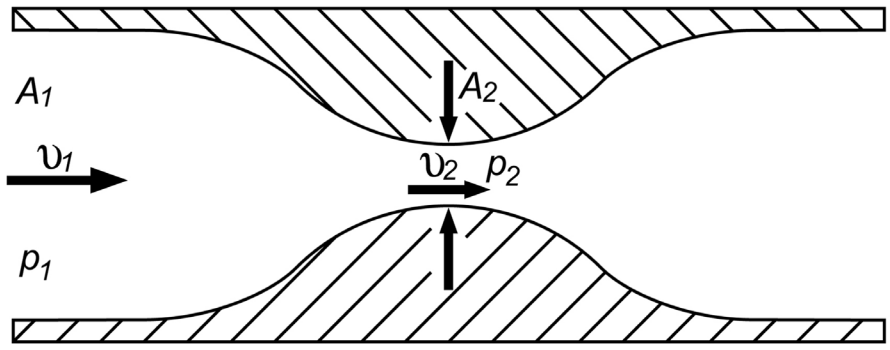

FIGURE 8.11: Blood vessel with a stenosis.

pressure is lower at the stenosed section of the blood vessel (the constriction) to ensure that the sum of the pressure and energy at each point along the blood vessel remains equal. The lower pressure at the stenosis makes the blood vessel with a stenosis more prone to collapse if an external pressure were applied to the blood vessel. Stents or drug -eluting stents may be inserted in an artery that has a stenosis to keep the artery open after the blockage has been cleared using angioplasty. Mass conservation shows that the velocity is higher at the stenosis due to a smaller area at the stenosis.

REYNOLD'S NUMBER

The Reynolds' number (Re) is a dimensionless number, which provides an indication of how blood is flowing in an artery. The Reynolds' number is given by:

$$\mathrm{Re} = \frac{UD\rho}{\mu}, \tag{15}$$

where U is the speed of the flow, D is the diameter of the blood vessel, ρ the blood density and μ the blood viscosity. For an artery, the flow tends to change from laminar to turbulent at a Reynolds' number of approximately 2000. This number should be treated as only a representative value, since the transition from laminar to turbulent flow may occur at higher Reynolds' numbers.

To see a representative peak value of Reynolds' number, we consider an abdominal aorta of diameter, D = 2.5 cm = 0.025 m, peak blood flow speed U = 60 cm/s = 0.6 m/s, blood density ρ = 1 gram/cc = 1000 kg/m^3 and blood viscosity μ = 0.0036 Pa s. These values give Re ≈ 4,200. So, in principle, it is possible for turbulent flow to occur in the aorta during the systolic phase.

Fluid flowing in a laminar fashion is dominated by the viscosity and at a high Reynolds' number by its inertia. A bruit is audible chaotic flow at high velocity with energy transformed to noise – inefficient flow that maybe disruptive as in a carotid stenosis – and blood needs to be able to flow fast in order to deliver its load at a cardiac output of up to 30L/min in an athlete.

Turbulent flow is less efficient relative to laminar flow. This means that more energy or a greater pressure drop is required to drive turbulent flow compared to laminar flow. A quantitative way of measuring this inefficiency is given by the formula for energy or "head" loss for flow along a pipe

$$h_L = f\,\frac{L}{D}\frac{U^2}{2g}, \tag{16}$$

where f is the loss coefficient, L the length of the artery or appropriate subsection of an artery and g the acceleration due to gravity. For laminar flow,

$$f_{lam} = \frac{64}{\mathrm{Re}}, \tag{17}$$

while for turbulent flow

$$f_{lturb} \sim \frac{0.316}{\mathrm{Re}^{1/4}}. \tag{18}$$

One can show that $f_{\mathrm{turb}} > f_{\mathrm{lam}}$ when Re > 1200, which implies that turbulence consumes more energy relative to laminar flow. This result is represented schematically in Figure 8.12, where we have plotted the ratio $f_{\mathrm{turb}}/f_{\mathrm{lam}}$ as a function of Re. Here we see that at a Reynolds' number of around 2000, turbulent flow loses 1.5 times more energy relative to laminar flow. As Re approaches 5000 turbulent flow tends to lose 3 times as much energy as laminar flow.

It is interesting to speculate that the particulate nature of blood and plasma composition may act to discourage the formation of turbulent flow. Each red cell, being bi-concave, could change the local interactions between the cells and the blood plasma so that the flow tends to remain laminar. The shape of the red cell then may enhance the efficiency of blood flow, in addi-

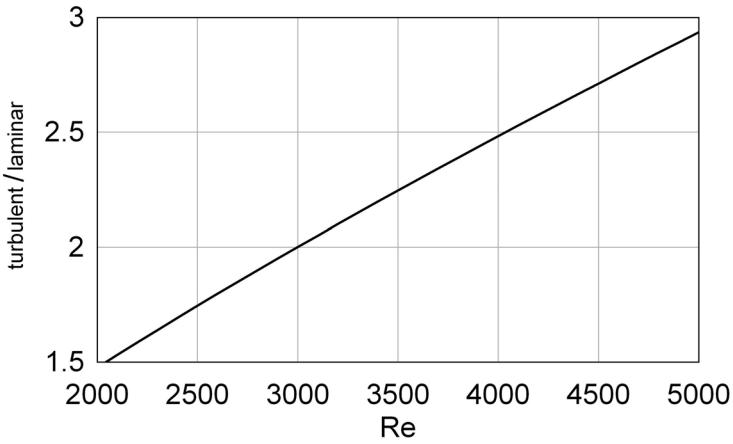

FIGURE 8.12: Plot of the ratio of turbulent to laminar energy loss coefficients.

tion to increasing surface area for oxygen delivery.

ARTERIAL DISSECTION, COLLATERAL CIRCULATION AND COMPETING FLOWS

To this point we have essentially discussed flow in series. Much of the normal flow and some pathological flow occurs in parallel. For example, the collateral circulation in each segment of the body; the profunda system in the thigh, the geniculate system around the knee and the tibial systems in the leg. Another good example is the carotid and vertebral systems combining to form the cerebral circulation. In parallel circulation, the pressure at the separation of the two systems is theoretically the same for each, and the pressure at the re-union is also the same for each. The proportion of ongoing flow from the two systems is determined by the resistance of each system. These two therefore compete for the proportion of on-flow. This works well to direct or redirect the flow to the target tissues. The body may select priorities for flow, for example, the brain and heart in shock or the muscles during exercise. The branches of the great vessels and arteries to the tissues are resistance vessels and they have muscular walls for this purpose. The formula for resistors in parallel circuits is

$$\frac{1}{R_{total}} = \frac{1}{R_1} + \frac{1}{R_2} + \ldots + \frac{1}{R_n}, \qquad (19)$$

where n is the number of parallel circuits.

These circuits also provide alternative channels should the dynamics change due to injury or disease. Not all parallel circuits are beneficial. Detrimental competing flows may occur with artificially created channels, for example, aorto-bifemoral bypass, when one iliac system is normal and the other occluded. The competing flows on the normal side predispose for either that limb of the graft or part of the iliac system on that side to occlude. Similarly, with femoro-popliteal bypass after long-standing superficial femoral artery occlusion when the profunda collateral flow has been well developed.

In aortic dissection, the outflow from the false lumen is met with greater resistance than the outflow from the true lumen. The flows compete where the intima has been torn off the origin of a branch vessel which therefore comes off the false lumen and leaves a hole in the membrane at that point. The pressure

is higher in the false lumen at any time in the cardiac cycle other than peak systole.

Figure 8.13 shows the trace from true and false lumens of a dissected aorta. Note the systolic pressure is same in each lumen at 138 mmHg. The diastolic is higher in the false lumen at 93 mmHg compared to the diastolic in the true lumen of 82 mmHg. The area under the curve is the same and so the pulse wave in the false lumen is wider. The mean pressure in the false lumen is higher at 109 mmHg than the true lumen where the mean is 91 mmHg.

This means that the false lumen is almost always the larger of the two and is more likely to dilate. Flow of contrast injected into the true lumen is not seen to flow out to the false lumen through the holes in the membrane unless the pressure of the injection and the pressure of the lumen together exceed the pressure of the false lumen. The membrane that is the remnant of the intima oscillates as the pressure ratio between the true and false lumen changes during the cardiac cycle. This dynamic also applies for a Type 1 endoleak into the residual sac of an aortic aneurysm treated by an endovascular graft.

SHEAR STRESS AND PRESSURE

All vascular clinicians are familiar with the ultimate shearing force injury of high velocity impact when the mobile arch of the aorta and heart continue to move forward while the descending aorta, held by the intercostals and posterior mediastinum, is held to the vertebral bodies. What of subtle persistent long-term shear stresses and the relationship with the greatest risk factor for arterial disease – age? There are known common sites for occlusive atheromatous plaques e.g. the carotid bifurcation, aortic bifurcation, origins of branches of the aorta and coronary arteries and shear stress points such as the adductor canal.

Atheroma is an arterial lesion. Occlusive and dilating diseases of the arteries progressively occur with ageing, and obviously age is the greatest risk factor. It is not seen in children and only seen in veins subject to long term pulsatile pressure when they are said to be "arterialised". For example, when a vein is used for an arterial bypass or for a dialysis fistula. Pressure and pulsatility are the forces involved. Persistent raised blood pressure above the norm causes progressive

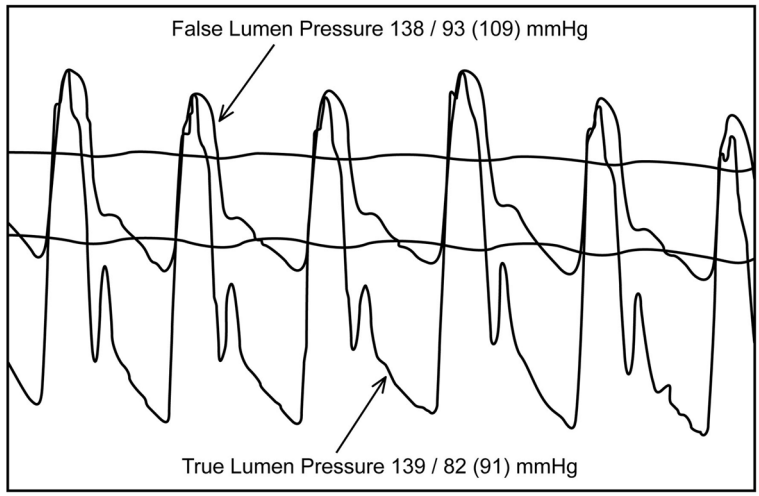

FIGURE 8.13: Pressure readings from the true and false lumens of a dissected abdominal aorta (courtesy of Dr John Anderson).

wall damage. With age there is degeneration of the wall of the artery and loss of compliance. Pulse pressure and peak systolic pressures rise because of the loss of compliance. Peaks of pressure occur with exertion and acute damage may occur at such times. Age will eventually affect all, but some are more genetically predisposed to arterial lesions and other risk factors such as poor diet and smoking accelerate any genetic predisposition.

Shear stress on an arterial wall, τ_w, due to Poiseuille fluid flow is given by the formula

$$\tau_w = \frac{4\mu q}{\pi a^3}, \qquad (20)$$

where a is the radius of the artery and q is the volume flow rate of blood through the artery. From this formula it can be seen that shear stress increases with the increase of blood flow through the artery and tends to increase as the artery becomes smaller in diameter – provided that the volume flow rate and the viscosity are approximately constant.

Atherosclerotic lesions form at specific areas where low and oscillatory endothelial shear stress occur. High risk plaques have a large lipid core, thin and inflamed fibrous cap and excessive expansive remodelling[9]. Wall shear stress may rupture the established plaque. Plaque rupture and intraplaque haemorrhage are recognized causes of cardiac events. Computational modelling of carotid bifurcations with atherosclerotic plaques that had patient-specific geometries obtained from Magnetic Resonance Imaging (MRI) scans and modelled the fluid-structure interactions have shown that stresses in the fibrous cap and around the plaque shoulders affect plaque rupture risk, with higher stress and plaque rupture risk for thinner caps.[10-13]

FORCES ON GRAFT SYSTEMS

The performance of endoluminal grafts (ELG) was found to be different to open repair with a sewn replacement of the artery because of unsuspected influences, as mentioned above, that relate to sustained physical forces.[1] The openly-sewn prosthesis binds the wall of the artery to the prosthesis with a transmural suture. The artery may expand above or below the prosthesis. However, at the point of attachment the artery wall is held to the fixed diameter by the through-wall suture for as long as the suture holds. ELG's to date do not bind the adventitia to the prosthesis – they merely attach. The ELG must continue to act to bridge the gap between normal artery above and below until, if ever, the aneurysm's cavity shrinks right down. In open surgery, the suture is binding and the tissues around supportive. The diameters of the grafts used for the same abdominal aortic aneurysm (AAA) differ markedly between the open and ELG methods. The common diameters used for tube replacement surgically of infrarenal AAA is 18 or 20 mm. The commonest diameter for an endoluminal graft is 26 or 28 mm and 30+ mm is not uncommon. Why such a discrepancy when the surgeon judges the diameter to suitable fit? This discrepancy is due to the different types of attachment of an open graft and an endoluminal graft. With the former, there are sutures through the graft and the full thickness of the aortic wall. This means that the aortic diameter at that point is permanently fixed to the diameter of the graft in its pressurised state. The diameter of a crimped vascular graft is, by definition, the minimum internal distance between the crimps in the non-pressurised state. It is increased by approximately 10% when pressurized. With the ELG, a residual radial force is required for seal and the attachment may or may not be enhanced by latching barbs. The oversize allowance must accommodate elasticity and compliance while maintaining the seal between pulsations for the whole of the length of the sealing zone.

These latching barbs sometimes cross the renal arteries but have been shown to have a minor effect of 1 % on the renal artery flow rate for 3 mm diameter artery.[14]

With an endoluminal graft the device must bridge a gap for an indeterminate time before the body reabsorbs the contents of the aneurysm and encases the graft in foreign body fibrous tissue support. Therefore the long term function and durability demands are different and more demanding.[1] Understanding the forces involved is basic to design and use of new technology and the weaknesses that lead to aneurysmal disease provides a challenge.[1,15]

A mistaken clinical impression is that the forces on a thoracic ELG should be greater than those on an abdominal ELG. The flow and diameter of the thoracic aorta are greater and the haemodynamic forces potentially much larger. However, because the diameter of the graft changes little, if at all, the downward displacement force in the thoracic ELG is small as the resistance in the graft is low – except on the aortic arch. The resistance of any graft that extends into the iliac vessels is much greater because of the significant change in diameter and high resistance within the graft acting like a windsock or sea anchor.[15] An aorto uni-iliac device affords greater resistance than a bifurcated graft and detachment at the neck and migration is a common problem due to high displacement forces. In contrast with the thoracic aorta there is little drag because there is little or no change in diameter. In contrast, there is little drag on a graft in the thoracic aorta because there is little or no change in diameter along the graft. The force applied to the graft is on the curve and centrifugal forces apply. Since every action has an equal and opposite reaction (Newton's third law), one must ask where is the reaction. The reaction is to pull the graft out from the top and the bottom almost equally. When endoluminal grafts were first used in the thorax, unexpected upward migration of the distal end emerged as the problem, especially when there was a significant curve on the graft. For the same reason, this 'lift out' may also be seen from the iliacs when the graft fixation is weak because of ectasia and/or short length of distal attachment. Type 1B endoleak can be more dangerous than Type 1A if this factor is ignored.

An important issue in vascular intervention is the durability of endoluminal grafts. Such grafts are often used to protect aneurysms from the effects of arterial pressure. Unfortunately, hemodynamic forces can displace a graft and thereby, potentially, interrupt the seal between the graft and the neck of the aneurysm. It is important, therefore to have an understanding of the possible forces that may be exerted on a graft.

To illustrate the steps used in determining the forces on a graft system, via analytic equations, we consider the steady flow of blood through a bent pipe (Figure 8.14). In this figure, the proximal inlet entrance is labelled by 1 and the distal exit by 2. D_1, A_1 and D_2, A_2 are the diameters and cross-sectional areas, respectively, of the graft at the points 1 and 2. The vector normals of the cross-sectional areas are, respectively, at angles of θ_1 and θ_2 to the vertical. Similarly p and $\boldsymbol{v}$ refer to the pressures and velocities at these points. R_x and R_y are the x and y components of the restoring force. The external pressure on the graft system is denoted by p_{ex}.

In our analysis, we assume steady-state, *i.e.*, non-pulsatile, flow. We do this as it gives us a basic idea of how the system is behaving.

The first equation is the steady-state **mass conservation** equation, which we rewrite in the form

$$v_1 A_1 = v_2 A_2. \tag{21}$$

One should note that v_1 and v_2 are average flow speeds, where the average is taken

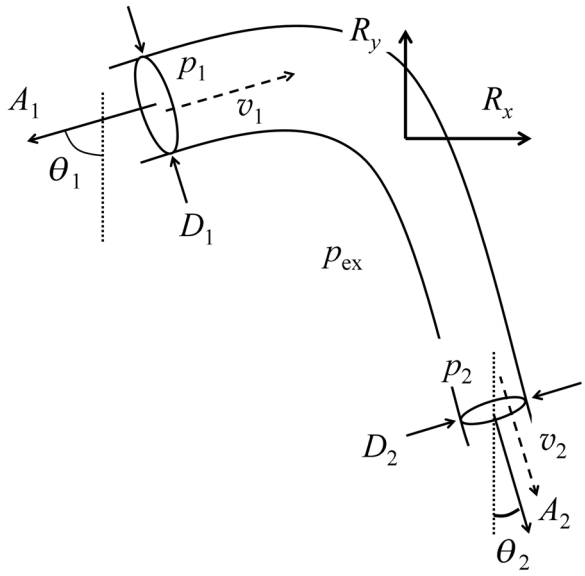

FIGURE 8.14: The characteristic velocity, pressure, area and force vectors required to compute the restraining forces on a bent, single-tube graft system.

over the areas of A_1 and A_2 respectively.

The next analysis tool at our disposal is the **momentum conservation** equation, which can be expressed in the form

$$R_x = \begin{matrix}(p_2 - p_{ex})A_2\sin\theta_2 - (p_1 - p_{ex})A_1\sin\theta_1 \\ + \rho v_2^2 A_2\sin\theta_2 - \rho v_1^2 A_1\sin\theta_1\end{matrix} \qquad (22)$$

and

$$R_y = \begin{matrix}-(p_1 - p_{ex})A_1\cos\theta_1 - (p_2 - p_{ex})A_2\cos\theta_2 \\ - \rho v_1^2 A_1\cos\theta_2 - \rho v_2^2 A_2\cos\theta_2\end{matrix} \qquad (23)$$

where in these formulae, we have ignored the weight of the graft and the weight of blood in the graft. These terms are easily included into the equations, if required.

Energy is the final conserved quantity that we can use in our analysis. The **energy conservation equation** has the form:

$$\frac{p_1}{\gamma} + \frac{\alpha_1 v_2}{2g} + z_1 = \frac{p_2}{\gamma} + \frac{\alpha_2 v_2^2}{2g} + z_2 + h_L\,, \qquad (24)$$

where g is the gravitational acceleration, $\gamma = \rho g$ is the weight density of blood, z_1 and z_2 are the vertical heights of the proximal and distal ends of the graft, respectively, and h_L is the 'head loss' in the pipe, *i.e.*, the amount of pressure or energy that is lost due to frictional viscous effects as the fluid travels through the pipe. Head loss is usually given by the equation

$$h_L = K_L \frac{v_2^2}{2g}\,, \qquad (25)$$

where K_L is a constant, the value of which is usually dependent on the shape, length and diameter of the pipe. The coefficients α_1 and α_2 are kinetic energy correction factors that have different values depending on the type of flow. For example, for uniform flow $\alpha = 1$, turbulent flow has $\alpha \approx 1$, and laminar flow gives $\alpha = 2$.

By combining Eqs (21), (24) and (25), one obtains

$$p_2 = p_1 + \frac{\gamma v_1^2}{2g}\left(\alpha_1 - (\alpha_2 + K_L)\left(\frac{A_1}{A_2}\right)^2\right) + \gamma(z_1 - z_2). \qquad (26)$$

So, by using Eqs (26) and (21), we can express p_2 and v_2 in terms of quantities at the entrance of the graft. This then allows us to compute the restraining forces on the graft system by then using Eqs (22) and (23).

Case 1 – The cylindrical graft

For this case, the inlet and the outlet areas are the same, so, by Eq. (21), the inlet and outlet flow speeds are also equal. The angles θ_1 and θ_2 are equal and have a value of 90°. The inlet and outlet pressures are not equal due to the frictional, shear interaction between the blood and the graft (*i.e.*, the head loss as given by Eq. (25)). This frictional interaction causes the outlet pressure, p_2, to be less than the inlet pressure, p_1. This is called a pressure drop.

From all of this information, one can write down the restraint forces on the graft. So, from Eqs (22) and (23):

$$R_y = 0, \tag{27}$$

i.e., there are no vertical forces generated by blood flowing through a horizontal graft and

$$R_x = (p_2 - p_1)A_1, \tag{28}$$

where we have set the external pressure to zero. In this case, the horizontal force on the graft is quite small, because p_1 will only be a little larger than p_2. One can conclude from this analysis that straight, cylindrical grafts only feel a relatively small drag force in the direction of the flow.

Case 2 – The windsock graft

Suppose now we consider a graft in the shape of a windsock, such as in Figure 8.16.

For this case, the inlet area is now larger than and the outlet area, so, by Eq. (21), the outlet flow speed is greater than the inlet flow speed as given by

$$v_2 = \left(\frac{A_1}{A_2}\right)v_1 \tag{29}$$

As in the previous case, the angles θ_1 and θ_2 are equal and have a value of 90° and the inlet and outlet pressures are not equal due to the frictional, shear interaction between the blood and the graft.

The restraint forces on the graft are from Eqs (22) and (23):

$$R_x = p_2A_2 - p_1A_1 + \rho v_2^2A_2 - \rho v_1^2A_1, \tag{30}$$

and

$$R_y = 0\ . \tag{31}$$

When you put in the appropriate numbers into Eq. (30), it is found that the dominant term in this equation is the p_1A_1 term. Many endoluminal grafts have this 'wind sock' shape with a distal exit area, which is smaller than the proximal, inlet area. This shape has a much larger drag force than for a cylindrical graft.

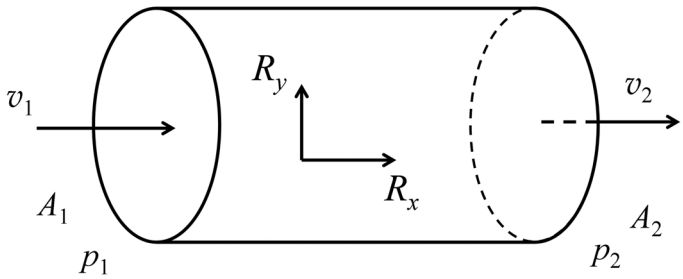

FIGURE 8.15: Cylindrical graft.

Case 3 – The curved graft

As with the cylindrical graft, the inlet and the outlet areas are the same, so, by Eq. (21), the inlet and outlet flow speeds are also equal. Due to the symmetry of the situation, the vertical restraint force is zero, the horizontal restraint force is given by

$$R_x = -p_2A_2 - p_1A_1 - pv_2^2A_2 - pv_1^2A_1 . \qquad (32)$$

So, now both the pressure and velocity components add together to produce a greater total force on the graft. This result suggests that a curved graft may be subject to greater forces than a wind-sock shaped graft.

Case 4 – The symmetric bifurcated graft

Suppose that we consider a symmetric bifurcated graft, such as shown in Figure 8.18, where the two outlet distal legs of the graft are at an angle α to the horizontal, the two distal ends are equal and gravity is ignored. The proximal end of the graft is labelled by the number 1, the symmetric distal ends by 2 and 3. By satisfying momentum conversation the horizontal restraint force is given by:

$$R_x = -p_1A_1 - 2p_2A_2\cos\alpha + pv_1^2A_1 - 2pv_2^2A_2\cos\alpha . \qquad (33)$$

The more general, non-symmetric case with gravity is described elsewhere.[15]

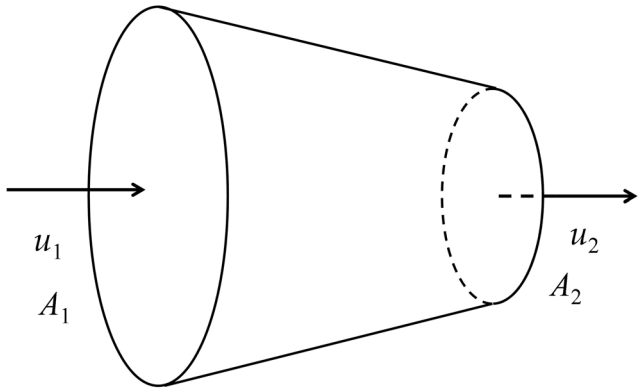

FIGURE 8.16: An endoluminal graft in the shape of a wind-sock.

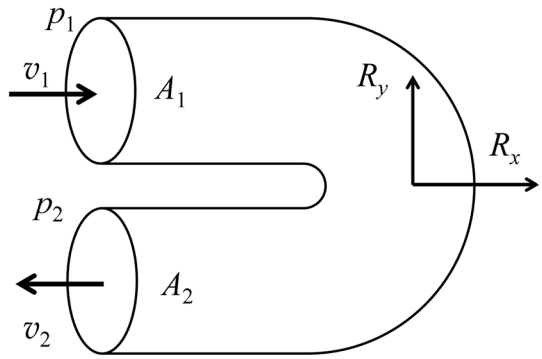

FIGURE 8.17: Curved graft.

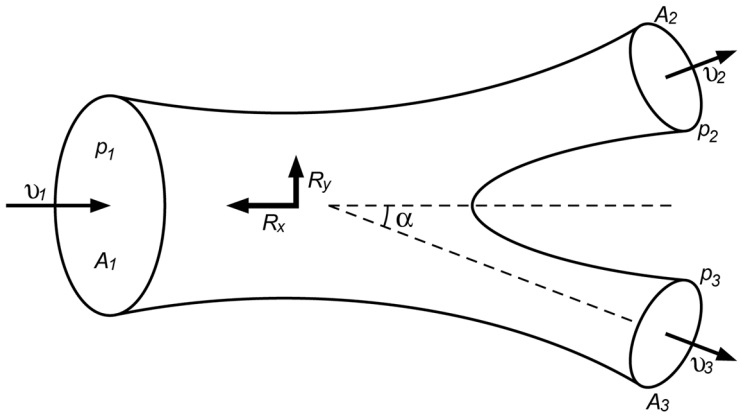

FIGURE 8.18: Symmetric bifurcated graft.

We also know to satisfy mass conversation that the flow in has to equal the sum of the outflows

$$v_1A_1 = v_2A_2 + v_3A_3, \tag{34}$$

and since it is a symmetric bifurcated graft then

$$v_1A_1 = 2v_2A_2. \tag{35}$$

By applying Bernoulli's equation 7 and mass conversation equation 35 then p_2 and v_2 can be eliminated from equation 33.

This equation shows that the horizontal restraint force is strongly dependent on inlet area, pressure and on the bifurcation angle (especially > 15°). But the blood inlet velocity or flow rate has negligible effect on the horizontal restraint force.[16-18] Naturally, a steady-state assumption is questionable, since pulsatile flow occurs in the human body. However, it was shown experimentally that a steady-state analytical model can be used, with variable pressure and flow rate inputs, to predict forces on a symmetric, bifurcated graft in pulsatile flow with reasonable approximation within design limits.[17-18] This steady-state analytical force model is now used in the design of grafts.

COMPUTATIONAL MODELLING

Computational fluid dynamics (CFD) and finite element modeling can assist in our understanding of vascular haemodynamics. CFD uses numerical methods to discretize and mesh the geometry and algorithms to solve the equations of motion (for example, the Navier-Stokes equation) and other relevant equations. In the last several years with advances in computing the computational modeling capability has greatly improved. It is now possible to incorporate patient-specific geometry from MRI, CT or magnetic resonance angiography (MRA) data. The computational models also now include fluid-structure interactions (fluid flow and wall deformation interaction), pulsatile flow and non-Newtonian flow. Some computational modelling of vascular haemodynamic systems include AAA grafts,[19-22] fluid-structure interactions with cerebral aneurysms,[23-25] patient-specific cerebral aneurysms with coils,[26-28] and patient-specific circle of

$$R_x = p_1A_1 - \rho\frac{A_1^2}{2A_2^2}v_1^2\cos\alpha + pv_1^2A_1 - 2A_2\left[p_1 + \frac{\rho}{2^2}v_1^2\left(1 - \frac{A_1^2}{2A_2^2}\right)\right]\cos\alpha\ . \tag{36}$$

Willis.[29-33] For example, Li and Kleinstreuer[19] modelled blood flow and structure interactions in a AAA with and without a graft where they incorporated fluid-structure interactions, flexible walls, pulsatile flow and non-Newtonian blood flow. They confirmed that the force on the graft is highly dependent on the diameter, blood pressure and bifurcation angle. They also showed significant reduction in AAA stress, displacement and pressure after graft placement as shown in Figure 8.19.

Endoleaks which are blood flow between graft and the AAA wall can also cause problems in AAA such as elevated sac pressure and high stresses which may lead to rupture. Li and Kleinstreuer[34] modelling analysis indicated the sac pressure caused by type II endoleaks (leakage via collateral arteries) depends on the inlet branch pressure; thus, type II endoleaks may increase sac pressure to near the systemic pressure levels, which could cause more clinical concern. Other studies have shown that intrasac pressure measurements and haemodynamic analysis of the graft-aortic wall interactions can be used to detect type II endoleaks.[35,36]

RECENT DEVELOPMENTS AND FUTURE DIRECTIONS

Mathematics, principles of physics and computational modelling of vascular haemodynamics have been useful in verifying or modifying intuitive engineering of endovascular stent grafts; and towards better understanding of failure modes of the cardiovascular system and its prostheses. For example, based on vascular haemodynamics analysis relating a vascular geometric ratio to the likelihood of aneurysm rupture, plaque rupture and stent graft migration.

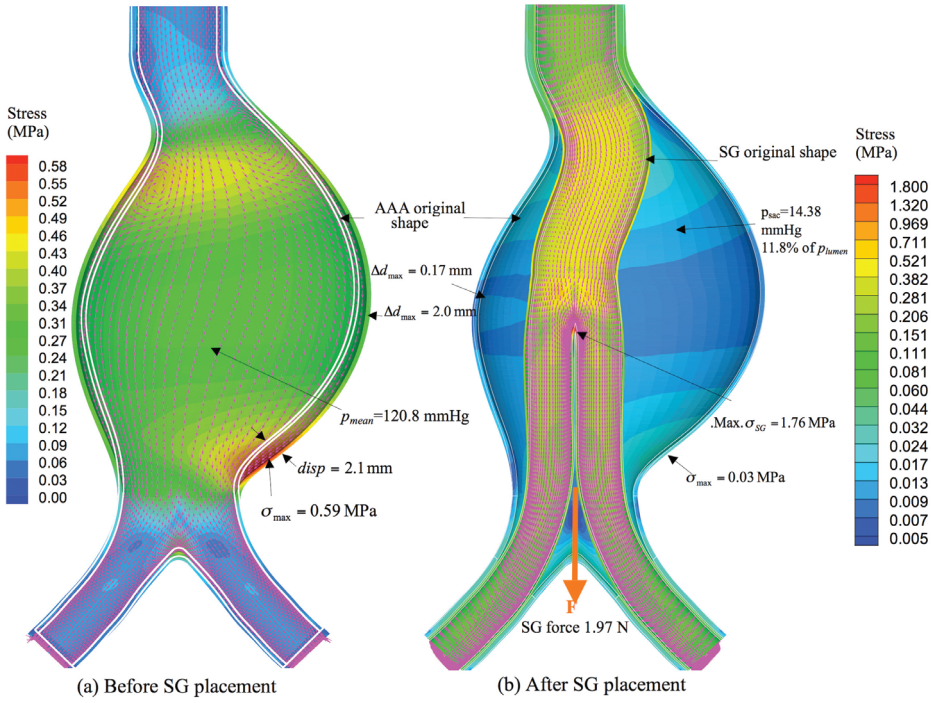

FIGURE 8.19: Effect of graft placement on blood flow and AAA wall at peak systole pressure level (courtesy of Professor Clement Kleinstreuer).[19]

CFD modelling of vascular haemodynamics is currently being used in the design and evaluation of implanted medical devices such as grafts. It is still a complex process to create patient-specific computational models and difficult for clinicians to interpret the results. In the future, computational modelling of vascular haemodynamics may be used as a tool for patient-specific blood flow quantification relevant to clinical practice to assist intervention planning, decision-making and optimization.

However, for computational modelling to be more easily translated to clinical relevance there needs to be more extensive comparisons of *in vitro* and *in vivo* clinical studies to validate the codes, with the uncertainties quantified, so they can be used with confidence. Patient-specific geometries and measured flow distribution boundary conditions should be included. There needs to be better models of arterial mechanical properties during each stage of a disease state (e.g. aneurysm formation), more accurate imaging techniques that can provide better information of the wall thicknesses, details on perivascular environment and much better coupling with vascular biology, mass transport and cellular biophysics. With grafts now being used in high curvature areas it is more important to understand the forces required to keep the grafts in place to mitigate their migration.

The intersect of clinical arterial pathology, feedback systems in physiology and computational fluid dynamics leads us to potentially the most exciting time in advances for arterial disease ever. The vascular system is dynamic in its function, its response to demand, its injury and repair cycle and its aging. The arterial system is intricately designed so that each arterial division is specific for its function and the demands placed upon it for up to one hundred years. To the empirical, statistical, biochemical, genetic and molecular biology knowledge of the cardiovascular system must be added the central role of haemodynamic physics and the pathology that results from the relentless forces of blood pressure and pulse wave. Modelling of arteries opens the door to much better understanding of why atheroma occurs at the known predictable sites such as the carotid bifurcation, the origins of branch vessels of the aorta and sites of stress for example the adductor canal.

CONCLUSION

Understanding the physics of the vascular system in health and disease will influence vascular management. This is a rich field for further research. Further clues to atherogenesis may lie in the differences of the fluid dynamics and stresses applied to the arterial systems. Computational modelling will be of increasing importance, as the science evolves, to our understanding of vascular haemodynamics.

REFERENCES

1. Lawrence-Brown MMD, Semmens JB, Hartley DE, Mun RP, van Schie G, Goodman MA, Prendergast FJ, Sieunarine K. How is Durability Related to Patient Selection and Graft Design with Endoluminal Grafting for Abdominal Aortic Aneurysm? *Durability of Vascular and Endovascular Surgery*. Edited by: R M Greenhalgh WB, Saunders 1999 375–385.
2. Harris PL, Buth J, Mialhe C, Myhre HO, Norgren L. The need for clinical trials of Endovascular abdominal aortic aneurysm stent-graft repair: The EUROSTAR project. *Journal of Endovascular Surgery* 1997; **4**: 72–77.
3. The UK Small Aneurysm Trial Participants. Mortality results for

randomized controlled trial of early elective surgery or ultrasonographic surveillance for small abdominal aortic aneurysms. *Lancet* 1998; **352**: 1649–55.
4. Lawrence-Brown MMD, Norman PE, Jamrozik K, Semmens JB, Donnelly NJ, Spencer C, Tuohy R. Initial Results of the Western Australian Ultrasound Screening Project for Aneurysm of the Abdominal Aorta: Relevance for Endoluminal Treatment of Aneurysm Disease. *Cardiovascular Surgery* 2001; **9**: 234–40.
5. Chien S., Usami S., Dellenbeck RJ, Gregersen M. Shear dependent deformation of erythrocytes in rheology of human blood. *Am J Physiol* 1970, **219**: 136–142.
6. A.S. Popel, P.C. Johnson, Microcirculation and hemorheology. *Annual Review of Fluid Mechanics,* **37** (2005), 43–69.
7. A. Pries, T. Secomb, P. Gaehtgens, Review—biophysical aspects of blood flow in the microvasculature. *Cardiovascular Research,* **32**: (1996), 654–667.
8. Barbee J. H. and Cokelet G. R. The Fahreus effect. *Microvascular Research* 1971 **34**: 6–21.
9. Y.S. Chatzizisis, A.U. Coskun, M. Jonas, E.R. Edelman, C.L. Feldman, P.H. Stone, Role of endothelial shear stress in the natural history of coronary atherosclerosis and vascular remodeling – Molecular, cellular, and vascular behaviour. *Journal of the American College of Cardiology*, **49:** (2007), 2379–2393.
10. H. Gao and Q. Long, Effects of varied lipid core volume and fibrous cap thickness on stress distribution in carotid arterial plaques. *Journal of Biomechanics*, **41**: (2008), 3053–3059.
11. S.A. Kock, J.V. Nygaard, N. Eldrup, E.T. Frund, A. Klaerke, W.P. Paaske, E. Falk and W.Y. Kim, Mechanical stresses in carotid plaques using MRI-based fluid–structure interaction models. *Journal of Biomechanics*, **41**: (2008), 1651–1658.
12. D. Tang, C. Yang, S. Mondal, F. Liu, G. Canton, T.S. Hatsukami and C. Yuan, A negative correlation between human carotid atherosclerotic plaque progression and plaque wall stress: in vivo MRI-based 2D/3D FSI models. *Journal of Biomechanics*, **41**: (2008), 727–736.
13. H. Gao, Q. Long, M. Graves, J.H. Gillard and Z.Y. Li, Carotid arterial plaque stress analysis using fluid–structure interactive simulation based on in-vivo magnetic resonance images of four patients. *Journal of Biomechanics,* **42**: (2009), 1416–1423.
14. K. Liffman, M.M.D. Lawrence-Brown, J.B. Semmens, I.D. Šutalo, A. Bui, F. White, and D.E. Hartley, Suprarenal fixation: effect on blood flow in an endoluminal stent wire across an arterial orifice. *Journal of Endovascular Therapy*, **10**: (2003), 260–274.
15. Liffman K, Lawrence-Brown MMD, Semmens JB, Bui A, Rudman M, Hartley D., Analytical modelling and numerical simulation of forces in an endoluminal graft. *Journal of Endovascular Therapy,* **8**: (2001), 358–371.
16. I.D. Šutalo, K. Liffman, M.M.D. Lawrence-Brown, and J.B. Semmens, Experimental force measurements on a bifurcated endoluminal stent-graft model – comparison with theory. *Vascular*, **13**: (2005), 98–106.
17. K. Liffman, I.D. Šutalo, A. Bui, M.M.D. Lawrence-Brown and J.B. Semmens, Experimental

Measurement and Mathematical Modelling of Pulsatile Forces on a Symmetric, Bifurcated Endoluminal Stent-Graft Model. *Vascular*, **17**: (2009), 201–209.
18. Zhou SN, How TV, Black RA, et al. Measurement of pulsatile haemodynamic forces in a model of a bifurcated stent graft for abdominal aortic aneurysm repair. *Proceedings of the Institution of Mechanical Engineers Part H-Journal of Engineering in Medicine*, **222**:(H4) (2008), 543–549.
19. Z. Li, C. Kleinstreuer, Analysis of biomechanical factors affecting stent-graft migration in an abdominal aortic aneurysm model. *Journal of Biomechanics*, **39**: (2006), 2264–2273.
20. Howell BA, Kim T, Cheer A, et al. Computational fluid dynamics within bifurcated abdominal aortic stent-grafts, *Journal of Endovascular Therapy,* **14**: (2007), 138–143.
21. Molony DS, Callanan A, Morris LG, et al., Geometrical Enhancements for Abdominal Aortic Stent-Grafts. *Journal of Endovascular Therapy*, **15**: (2008), 518–529.
22. Figueroa CA, Taylor CA, Yeh V, et al., Effect of Curvature on Displacement Forces Acting on Aortic Endografts: A 3-Dimensional Computational Analysis, Thoracic. *Journal of Endovascular Therapy*, **16**: (2009), 284–294.
23. Torii R, Oshima M, Kobayashi T, Takagi K, Tezduyar TE. Fluid-structure interaction modeling of a patient-specific cerebral aneurysm: influence of structural modeling. *Computational Mechanics*, **43**: (2008), 151–159.
24. Valencia A, Solis F. Blood flow dynamics and arterial wall interaction in a saccular aneurysm model of the basilar artery. *Computers and Structures*, **84**: (2006), 1326–37.
25. Tezduyar TE, Sathe S, Cragin T, Nanna B, Conklin BS, Pausewang J, Schwaab M, Modelling of fluid-structure interactions with the space-time finite elements: Arterial fluid mechanics, *International Journal for Numerical Methods in Fluids*, **54**: (2007), 901–922.
26. Kakalis NMP, Mitsos AP, Byrne JV, Ventikos Y. The haemodynamics of endovascular aneurysm treatment: A computational modelling approach for estimating the influence of multiple coil deployment. *IEEE Transactions on Medical Imaging*, **27**: (2008), 814–824.
27. Canton G, Levy DI, Lasheras JC. Changes of intra-aneurysmal pressure during coiling: reply. *American Journal of Neuroradiology*, **27**: (2006), 472–4.
28. Cebral JR, Lohner R. Efficient simulation of blood flow past complex endovascular devices using an adaptive embedding technique. IEEE Transactions on Medical Imaging, **24**: (2005), 468–76.
29. Alnaes, M.S., Isaksen, J., Mardal, K.A., Romner, B., Morgan, M.K., Ingebrigtsen, T., Computation of hemodynamics in the circle of Willis. *Stroke,* **38**: (2007), 2500–2505.
30. Grinberg, L., Anor, T., Madsen, J.R., Yakhot, A., Karniadakis, G.E., Large-Scale Simulation of The Human Arterial Tree. *Clinical and Experimental Pharmacology and Physiology*, **36**: (2009), 194–205.
31. Kim, C.S., Numerical simulation of auto-regulation and collateral circulation in the human brain. *Journal of Mechanical Science and Technology*, **21**: (2007), 525–535.
32. Moore, S., David, T., Chase, J.G., Arnold, J., Fink, J., 3D models of

blood flow in the cerebral vasculature. *Journal of Biomechanics*, **39**: (2006), 1454–1463.
33. Šutalo, I.D., Bui, .A, Ahmed, S., Liffman, K., Manasseh, R. 2009. Modelling of flow through the circle of Willis and cerebral vasculature. Modelling in Medicine and Biology VIII, WIT Transactions on Biomedicine and Health, Vol. 13., BioMED 2009, WIT Press, (2009), 83–92.
34. Z. Li, C. Kleinstreuer, Computational analysis of type II endoleaks in a stented abdominal aortic aneurysm model, *Journal of Biomechanics*, **39**: (2006), 2573–2582.
35. K. Liffman, I.D. Šutalo, M.M.D. Lawrence-Brown, J.B. Semmens, B. Aldham, Movement and dislocation of Modular stent-grafts due to pulsatile flow and the pressure difference between the stent-graft and aneurysm sac. *Journal of Endovascular Therapy*, **13**: (2006), 51–61.
36. M.M.D. Lawrence-Brown, Z. Sun, J.B. Semmens, K. Liffman, I.D. Šutalo, D. B. Hartley, Type II endoleaks: When is intervention indicated and what is the index of suspicion for Types I or III? *Journal of Endovascular Therapy*, **16**: (Suppl. I)

Cover design by Emma Spoehr

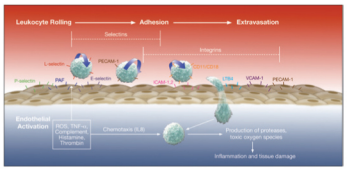

Cover diagram by David Heinrich of the *Medical Illustration and Media Unit, Flinders Medical Centre*. (See chapter 18)

Mechanisms of Vascular Disease

Edited by Robert Fitridge and Matthew Thompson

Chapter 1: Endothelium **Chapter 2:** Vascular smooth muscle structure and function **Chapter 3:** Atherosclerosis **Chapter 4:** Mechanisms of plaque rupture **Chapter 5:** Current and emerging therapies in atheroprotection **Chapter 6:** Molecular approaches to revascularisation in peripheral vascular disease **Chapter 7:** Biology of restenosis and targets for intervention **Chapter 8:** Vascular arterial haemodynamics **Chapter 9:** Physiological haemostasis **Chapter 10:** Hypercoagulable states **Chapter 11:** Platelets in the pathogenesis of vascular disease and their role as a therapeutic target **Chapter 12:** Pathogenesis of aortic aneurysms **Chapter 13:** Pharmacological treatment of aneurysms **Chapter 14:** Aortic dissection and connective tissue disorders **Chapter 15:** Biomarkers in vascular disease **Chapter 16:** Pathophysiology and principles of management of vasculitis and Raynaud's phenomenon **Chapter 17:** SIRS, sepsis and multiorgan failure **Chapter 18:** Pathophysiology of reperfusion injury **Chapter 19:** Compartment syndrome **Chapter 20:** Pathophysiology of pain **Chapter 21:** Postamputation pain **Chapter 22:** Treatment of neuropathic pain **Chapter 23:** Principles of wound healing **Chapter 24:** Pathophysiology and principles of varicose veins **Chapter 25:** Chronic venous insufficiency and leg ulceration: Principles and vascular biology **Chapter 26:** Pathophysiology and principles of management of the diabetic foot **Chapter 27:** Lymphoedema – Principles, genetics and pathophysiology **Chapter 28:** Graft materials past and future **Chapter 29:** Pathophysiology of vascular graft infections

BARR SMITH PRESS

An imprint of
The University of Adelaide Press